

RISE-Based Adaptive Control with Mass-Inertia Parameter Estimation for Aerial Transportation of Multi-Rotor UAVs

Shuyang Shi, Yuzhu Li, Wei Dong

Abstract—This paper proposes an adaptive tracking strategy with mass-inertia estimation for aerial transportation problems of multi-rotor UAVs. The dynamic model of multi-rotor UAVs with disturbances is firstly developed with a linearly parameterized form. Subsequently, a cascade controller with the robust integral of the sign of the error (RISE) terms is applied to smooth the control inputs and address bounded disturbances. Then, adaptive estimation laws for mass-inertia parameters are designed based on a filter operation. Such operation is introduced to extract estimation errors exploited to theoretically guarantee the finite-time (FT) convergence of estimation errors. Finally, simulations are conducted to verify the effectiveness of the designed controller. The results show that the proposed method provides better tracking and estimation performance than traditional adaptive controllers based on sliding mode control algorithms and gradient-based estimation strategies.

Index Terms—Multi-rotor UAVs, aerial transportation, adaptive control, RISE, mass-inertia estimation.

I. INTRODUCTION

In recent years, unmanned aerial vehicles (UAVs), especially multi-rotor UAVs, have been widely applied to military/civil transportation tasks such as parcel delivery [1], equipment deployment [2], and rescue missions [3]. These tasks share common characteristics that the mass-inertia parameters of UAVs vary from flight to flight, and a fine-tune of controllers to retain good tracking performances between missions is time-consuming [4]. Thus, the varying, namely, the uncertain mass-inertia parameters, can be problematic for the control of UAVs [5]. Meanwhile, these light and flexible UAVs are susceptible to external disturbances such as winds [6], which seriously degrades flight performances.

To maintain good flight performance of multi-rotor UAVs and better conduct transportation missions, researchers have proposed different control methods to reduce the influence of uncertain mass-inertia parameters and disturbances, such as PID control [7], [8], backstepping control [9], and sliding mode control (SMC) [10], just to enumerate a few. These controllers incorporate mass-inertia changes caused by different loads into disturbances [11] and compensate for the overall disturbances via different methods. For instance, [7] studied the stability of UAVs with dynamic load disturbances and improved the control performance by careful selection of control gains. [10] proposed a non-singular terminal sliding mode controller with high-order sliding mode observers to address uncertain parameters and disturbances.

While incorporating mass-inertia uncertainties into disturbances is generally effective, improvements are possible. In aerial transportation problems, the variable mass-inertia parameters of loads take a large proportion of the UAV self-

parameters, but the ability of the above controllers to accommodate for such variation is moderate [12]. To tackle such problems, adaptive controllers with mass-inertia estimation have been considered. These controllers provide mass-inertia estimation [13] to improve dynamic models while addressing external disturbances. Hence, dynamic models can be corrected after UAVs take off with new loads, yielding better tracking performances [14], [15]. For instance, Mellinger *et al.* [16] proposed an adaptive PID control method that estimates payload parameters during hover via the least-squares methods. In [17], an adaptive cascade controller was designed with the estimation of external force and position of the center of mass. [18] established a complete dynamics model of quadrotors and proposed an adaptive controller based on feedback linearization and mass-inertia estimation. Bouadi *et al.* [13] addressed a SMC algorithm with consideration of white Gaussian noise and mass-inertia uncertainties. [19] designed a learning rate-based SMC controller with the estimation of the mass of variable loads for altitude control. [20] proposed a finite-time sliding mode controller for disturbance rejection and an adaptive-tuning scheme for mass estimation. In [21], no prior knowledge of uncertain parameters was required via adaptive estimation laws based on signum and saturation functions. [22] designed a non-singular fast terminal sliding mode controller based on adaptive integral backstepping to overcome external disturbances and an adaptive estimation algorithm to estimate the variable mass of loads.

However, the methods mentioned can still be improved in two aspects. Firstly, the parameter estimation performance is influenced by disturbances. The convergence of estimation error can not be guaranteed via traditional least-squares [16] or gradient-based [18] algorithms when external disturbance exists. These methods are sensitive to disturbances and may trigger bursting phenomena, i.e., the estimated parameters may go to infinity, leading to the instability of the system [23]. In some improved gradient-based methods, the boundedness of estimation error is retained, but the error convergence can not be achieved [17], [13]. In [19]~[22], the estimation gradient is determined by high-order tracking errors, which makes the convergence speed easily interfered by external disturbances. Secondly, the performances of controllers are degraded in practical applications. While SMC has been exploited in [21] to address the influence of environmental disturbances, the performance in practical application is not satisfactory enough. The chattering phenomena of sliding mode controllers make the control input signal unreachable physically [19], which significantly degrades the control

performances. In [20], [22], such phenomena are restrained via continuous terms in sliding surfaces [22], but the rapid-changing amplitude of control input signals are still hard to achieve in physical systems.

Given the discussion above, this article proposes a new adaptive control method with mass-inertia estimation and disturbance rejection for aerial transportation tasks of multi-rotor UAVs. A RISE term [24] is applied for smoothing control inputs of the controller and disturbance rejection. A filter operation [25] is introduced to extract estimation errors exploited to guarantee the FT convergence of estimation errors theoretically. Then adaptive estimation laws are designed based on the extracted history estimation errors.

The major contributions of our work are summarized as follows:

- 1) An adaptive control method based on RISE terms is formulated with mass-inertia estimation. The scheme guarantees the asymptotic convergence of tracking error and FT convergence of estimated parameters under disturbances and provides smooth control input signals achievable in practical applications.
- 2) The effectiveness of the proposed method is verified through comparative simulation results with MATLAB.

The rest of this article is organized as follows. A mathematical model of the studied multirotor system is described in Section II. Section III provides the cascade controller design and Section IV formulates the parameter update law. Afterward, stability analysis is conducted in Section V. Section VI presents comparative simulation results. Finally, conclusions are drawn in Section VII.

II. DYNAMIC MODEL

To develop the dynamic model of UAV, the definition of frames is first given as is shown in the following figure. The inertial frame (the earth frame) $\{E\}$ is fixed on the ground and the body fixed frame $\{B\}$ is chosen to coincide with the geometric center of the UAV. Let $\eta_1 \triangleq [x \ y \ z]^T \in \mathbb{R}^3$ denote the position of the origin of $\{B\}$ and $\eta_2 \triangleq [\phi \ \theta \ \psi]^T \in \mathbb{R}^3$ represent the three Euler angles roll, pitch and yaw in frame $\{E\}$. In order to simplify the model, the CoG is assumed to be fixed in $\{B\}$ when loads changes [19]. Ignoring the asymmetry of the multi-rotor UAV and according to the Newton-Euler formalism, the rigid body dynamics model used in the subsequent controller design and stability analysis are governed by

$$\begin{cases} m\ddot{\eta}_1 = F - \begin{bmatrix} 0 \\ 0 \\ mg \end{bmatrix} - \Delta_1 \\ J\ddot{\eta}_2 = \tau_B - \dot{\eta}_2 \times J\dot{\eta}_2 - \Delta_2 \end{cases} \quad (1)$$

where $m \in \mathbb{R}$ represents the unknown mass of the multirotor; $J \in \mathbb{R}^{3 \times 3}$ is a matrix representing unknown moment of inertia of the multirotor about the origin of $\{B\}$. Its non-diagonal elements are set to be zero due to the symmetry of the UAV. $F \in \mathbb{R}^3$ denotes the multirotor force vector expressed in frame $\{E\}$ and $\tau_B \in \mathbb{R}^3$ denotes the torque expressed in frame $\{B\}$.

$\Delta_1 \in \mathbb{R}^3$ and $\Delta_2 \in \mathbb{R}^3$ are defined to express the unknown additive nonlinear disturbances. Equation (1) can be partly simplified and rewritten into a more compact form

$$\begin{cases} m\ddot{\eta}_1 + G + \Delta_1 = F \\ J\ddot{\eta}_2 + C(\dot{\eta}_2)\dot{\eta}_2 + \Delta_2 = \tau_B \end{cases} \quad (2)$$

by defining $C(\dot{\eta}_2) \triangleq -S(J\dot{\eta}_2) \in \mathbb{R}^{3 \times 3}$ and $G \triangleq [0 \ 0 \ mg]^T \in \mathbb{R}^3$, where $S(\cdot) \in \mathbb{R}^{3 \times 3}$ represents the skew symmetric matrix of a vector. The rewritten equation (2) is still in a separate form because the following controller and parameter update law design are developed in a cascade manner.

There are several properties and assumptions of the dynamics model which will be exploited in the subsequent development:

Property 1. Part of the dynamics equation (2) can be linearly parameterized as

$$\begin{cases} \Psi_1 \theta_1 \triangleq m\ddot{\eta}_1 + G \\ \Psi_2 \theta_2 \triangleq J\ddot{\eta}_2 + C(\dot{\eta}_2)\dot{\eta}_2 \end{cases} \quad (3)$$

where $\theta_1 \in \mathbb{R}$ and $\theta_2 \in \mathbb{R}^{3 \times 3}$ contain the unknown system mass-inertia parameters, $\Psi_1(\dot{\eta}_1) \in \mathbb{R}^3$ and $\Psi_2(\dot{\eta}_2, \ddot{\eta}_2) \in \mathbb{R}^{3 \times 3}$ are the regression matrices which contains known functions of measured acceleration, angular rate and angular acceleration respectively. The above linearization can also be formulated with desired position and attitude vectors, yielding

$$\begin{cases} \Psi_{1d} \theta_1 \triangleq m\ddot{\eta}_{1d} + G \\ \Psi_{2d} \theta_2 \triangleq J\ddot{\eta}_{2d} + C(\dot{\eta}_{2d})\dot{\eta}_{2d} \end{cases} \quad (4)$$

where $\Psi_{1d}(\ddot{\eta}_{1d}) \in \mathbb{R}^3$ and $\Psi_{2d}(\ddot{\eta}_{2d}, \dot{\eta}_{2d}) \in \mathbb{R}^{3 \times 3}$ are bounded desired regression matrices containing known functions of desired tracking vectors respectively.

Assumption 1. The regression matrices Ψ_{1d} and Ψ_{2d} defined above satisfy the PE condition described in [26], which can be easily fulfilled in our experiments. And the condition is important for the parameter update law given later in the article.

Assumption 2. The nonlinear disturbances Δ_1 and Δ_2 and their first two-order time derivatives, i.e. $\dot{\Delta}_i, \ddot{\Delta}_i, (i = 1, 2)$ are bounded by known constants.

III. CONTROL DESIGN

The control objective is to design a controller which guarantees that the system tracks a desired trajectory η_{1d} and ψ_d despite the bounded disturbances and uncertain parameters in the dynamics model. The desired trajectory η_{1d} and ψ_d are designed such that $\eta_{1d}^{(i)}(t)$ and $\psi_d^{(i)}(t)$, $i = 0, 1, \dots, 4$ exist and are bounded.

The controller illustrated in 1 is constructed with a cascade structure consisting of an outer-loop controller and an inner-loop controller. The outer-loop controller generates the thrust F and desired roll, pitch angles to track the desired position trajectory and yaw angle. The inner-loop controller is designed to generate the torque T needed to track the desired yaw angle and the calculated roll and pitch angle trajectories.

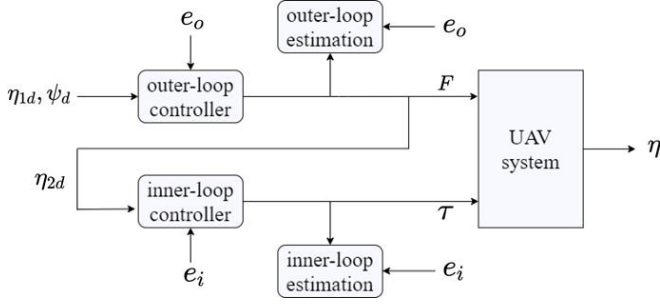


Fig. 1. Controller

A. Outer-Loop Controller

To quantify the control performance, tracking error $e_{o1} \in \mathbb{R}^3$, and two auxiliary filtered tracking errors $e_{o2} \in \mathbb{R}^3$ and $r_o \in \mathbb{R}^3$ are defined as follows:

$$\begin{aligned} e_{o1} &\triangleq \eta_{1d} - \eta_1, \\ e_{o2} &\triangleq \dot{e}_{o1} + k_{o1}e_{o1}, \\ r_o &\triangleq \dot{e}_{o2} + k_{o2}e_{o2}, \end{aligned} \quad (5)$$

where $k_{o1}, k_{o2} \in \mathbb{R}^+$ are designed constant control gains. By substituting the errors in (5) and the linearized form 4 into the first dynamic equation in (2), the open-loop error dynamics of outer-loop system can be developed as:

$$mr_o = \Psi_{1d}\theta_1 + S_1 + \Delta_1 - F \quad (6)$$

where the auxiliary function $S_1 \in \mathbb{R}^3$ is defined as

$$S_1 \triangleq m(k_{o1}\dot{e}_{o1} + k_{o2}\dot{e}_{o2}) \quad (7)$$

The output force F can be designed with an adaptive feedforward term and a RISE feedback term as

$$F \triangleq \Psi_{1d}\hat{\theta}_1 + \mu_1 \quad (8)$$

In (8), $\hat{\theta}_1 \in \mathbb{R}$ denotes the adaptive estimate for the unknown parameter θ_1 whose implementation will be discussed with detail in Section IV later. $\mu_1 \in \mathbb{R}^3$ represents the RISE feedback term described in [27], which is designed as

$$\begin{aligned} \mu_1 &\triangleq (k_{s1} + 1)e_{o2} - (k_{s1} + 1)e_{o2}(0) \\ &\quad + \int_0^t [(k_{s1} + 1)k_{o2}e_{o2}(\tau) + \beta_o \text{sgn}(e_{o2}(\tau))] d\tau \end{aligned} \quad (9)$$

where $k_{s1} \in \mathbb{R}^+$ and $\beta_o \in \mathbb{R}^+$ are constant control gains and $\text{sgn}(\cdot)$ represents the signum function. Then the time derivative of the RISE term can be derived as

$$\dot{\mu}_1 = (k_{s1} + 1)r_o + \beta_o \text{sgn}(e_{o2}) \quad (10)$$

Substituting equation (8) into (6), the closed-loop error dynamics of outer-loop system can be developed as

$$mr_o = \Psi_{1d}\tilde{\theta}_1 + S_1 + \Delta_1 - \mu_1 \quad (11)$$

where $\tilde{\theta}_1 \triangleq \theta_1 - \hat{\theta}_1 \in \mathbb{R}$ denotes the parameter estimation error. Equation (11) will be exploited in Section V to facilitate stability analysis of outer-loop controller.

The desired body attitude in frame $\{E\}$ then can be derived in the same manner as [28], by first calculating the desired

z-axis direction of the body frame $\{B\}$, which is alone the desired output force F :

$$\mathbf{z}_B = \frac{F}{\|F\|} \quad (12)$$

where $\|\cdot\|$ denotes the Euclidean norm. $\|F\|$ will be nonzero to avoid free-falling. Given the desired yaw angle ψ_d , a unit vector $\mathbf{x}_C \in \mathbb{R}^3$ can be defined as

$$\mathbf{x}_C \triangleq [-s\psi_d \quad c\psi_d \quad 0]^T \quad (13)$$

where $s\psi_d$ and $c\psi_d$ denotes $\sin(\psi_d)$ and $\cos(\psi_d)$ respectively. Provided $\mathbf{x}_C \times \mathbf{z}_B \neq 0$, the orientation of frame $\{B\}$ can be uniquely determined as

$$\begin{aligned} \mathbf{x}_B &= \frac{\mathbf{x}_C \times \mathbf{z}_B}{\|\mathbf{x}_C \times \mathbf{z}_B\|} \\ \mathbf{y}_B &= \mathbf{z}_B \times \mathbf{x}_B \\ \mathbf{R}_B^E &\triangleq [\mathbf{x}_B \quad \mathbf{y}_B \quad \mathbf{z}_B] \end{aligned} \quad (14)$$

where \mathbf{x}_B and \mathbf{y}_B are x and y axes of frame $\{B\}$ respectively. $\mathbf{R}_B^E \in \mathbb{R}^{3 \times 3}$ is the rotation matrix from the body-fixed frame $\{B\}$ to the inertial frame $\{E\}$, given by

$$\mathbf{R}_B^E = \begin{bmatrix} c\psi c\vartheta & c\psi s\vartheta s\phi - s\psi c\phi & c\psi s\vartheta c\phi + s\psi s\phi \\ s\psi c\vartheta & s\psi s\vartheta s\phi + c\psi c\phi & s\psi s\vartheta c\phi - c\psi s\phi \\ -s\vartheta & c\vartheta s\phi & c\vartheta c\phi \end{bmatrix} \quad (15)$$

The desired roll angle ϕ_d and pitch angle θ_d can be calculated from ψ_d and F via equations (12), (13), (14) and (15).

B. Inner-Loop Controller

The realization of inner loop controller is similar to that of the outer controller. First, tracking error $e_{i1} \in \mathbb{R}^3$ and auxiliary filtered errors $e_{i2}, r_i \in \mathbb{R}^3$ are defined as

$$\begin{aligned} e_{i1} &\triangleq \eta_{2d} - \eta_2, \\ e_{i2} &\triangleq \dot{e}_{i1} + k_{i1}e_{i1}, \\ r_i &\triangleq \dot{e}_{i2} + k_{i2}e_{i2}, \end{aligned} \quad (16)$$

where $k_{i1} \in \mathbb{R}$ and $k_{i2} \in \mathbb{R}$ are constant control gains. By substituting the errors in (16) and the linearized form 4 into the second equation in (2), the open-loop error dynamics of outer-loop system can be developed as:

$$Jr_i = \Psi_{2d}\theta_2 + S_2 + \Delta_2 - \tau_B \quad (17)$$

where the auxiliary function $S_2 \in \mathbb{R}^3$ is defined as

$$S_2 \triangleq J(k_{i1}\dot{e}_{i1} + k_{i2}\dot{e}_{i2}) + C(\dot{\eta}_2)\dot{\eta}_2 - C(\dot{\eta}_{2d})\dot{\eta}_{2d} \quad (18)$$

The inner-loop control output T can be designed with an adaptive feedforward term and a RISE feedback term as

$$\tau_B \triangleq \Psi_{2d}\hat{\theta}_2 + \mu_2 \quad (19)$$

In (19), $\hat{\theta}_2 \in \mathbb{R}$ denotes the adaptive estimate for the unknown parameter θ_2 ; $\mu_2 \in \mathbb{R}^3$ represents the RISE feedback term and is designed similar to equation (9) as

$$\begin{aligned} \mu_2 &\triangleq (k_{s2} + 1)e_{i2} - (k_{s2} + 1)e_{i2}(0) \\ &\quad + \int_0^t [(k_{s2} + 1)k_{i2}e_{i2}(\tau) + \beta_i \text{sgn}(e_{i2}(\tau))] d\tau \end{aligned} \quad (20)$$

and its time derivative similar to (10) as

$$\dot{\mu}_2 = (k_{s2} + 1)r_i + \beta_i \text{sgn}(e_{i2}) \quad (21)$$

where $k_{s2} \in \mathbb{R}^+$ and $\beta_i \in \mathbb{R}^+$ are constant control gains. Substituting equation (19) into (17), the closed-loop error dynamics of outer-loop system can be developed as

$$Jr_i = \Psi_{2d}\tilde{\theta}_2 + S_2 + \Delta_2 - \mu_2 \quad (22)$$

where $\tilde{\theta}_2 \triangleq \theta_2 - \hat{\theta}_2 \in \mathbb{R}^3$ denotes the parameter estimation error. Equation (22) will be exploited in Section V to facilitate stability analysis of inner-loop controller.

IV. PARAMETER ESTIMATION

The parameter estimation is conducted in both of the control loops with the same error extraction process. In the outer-loop, $\hat{\theta}_1$ is calculated and exploited to generate control outputs, $\hat{\theta}_2$ in the inner-loop respectively.

A. Estimation In Outer-Loop

The estimation starts with the definition of two filtered auxiliary vectors $F_f, \Psi_{1f} \in \mathbb{R}^3$ as the solutions to the following equation

$$\begin{cases} \alpha_1 \dot{F}_f + F_f = F, & F_f(0) = \mathbf{0} \\ \alpha_1 \dot{\Psi}_{1f} + \Psi_{1f} = \Psi_1, & \Psi_{1f}(0) = \mathbf{0} \end{cases} \quad (23)$$

where $\alpha_1 \in \mathbb{R}^+$ is a designed constant. Another filtered variable only used for analysis $\Delta_{1f} \in \mathbb{R}^3$ is also defined as

$$\alpha_1 \dot{\Delta}_{1f} + \Delta_{1f} = \Delta_1, \quad \Delta_{1f}(0) = \mathbf{0} \quad (24)$$

where Δ_{1f} is bounded given that Δ_1 is bounded. (23) and (24) actually exert the same low-pass filter operation on both sides of the linearized dynamic model

$$\Psi_1 \theta_1 + \Delta_1 = F \quad (25)$$

Then a filtered form of the above equation can be expressed as

$$\Psi_{1f} \theta_1 + \Delta_{1f} = F_f \quad (26)$$

To extract the estimation error $\tilde{\theta}_1$, $P_1, Q_1 \in \mathbb{R}$ are defined as

$$\begin{cases} P_1 \triangleq \int_0^t e^{-l_1(t-\tau)} \Psi_{1f}^T(\tau) \Psi_{1f}(\tau) d\tau + \varrho_1 \\ Q_1 \triangleq \int_0^t e^{-l_1(t-\tau)} \Psi_{1f}^T(\tau) F_f(\tau) d\tau \end{cases} \quad (27)$$

which are the solutions to the equation below

$$\begin{cases} \dot{P}_1 = -l_1 P_1 + \Psi_{1f}^T \Psi_{1f}, & P_1(0) = \varrho_1 \\ \dot{Q}_1 = -l_1 Q_1 + \Psi_{1f}^T F_f, & Q_1(0) = 0 \end{cases} \quad (28)$$

where $l_1 \in \mathbb{R}^+$ is a designed constant, and $\varrho_1 \in \mathbb{R}^+$ is a positive constant selected to ensure $P_1(0)$ is invertible at time $t = 0$. Such definition of P_1 yields the following property:

Property 3. P_1 is a positive variable satisfying $0 < \varrho_1 < P_1$. Then P_1^{-1} is globally invertible provided that the offset value ϱ_1 is not selected as 0. The proof of this property is similar to that of [25].

Similar to P_1 and Q_1 , $\bar{\Delta}_1 \in \mathbb{R}$ is defined as

$$\bar{\Delta}_1 \triangleq - \int_0^t e^{-l_1(t-\tau)} \Psi_{1f}^T(\tau) \Delta_1 d\tau + \varrho_1 \theta_1 \quad (29)$$

which is bounded by $\|\bar{\Delta}_1\| \leq \xi_{\Delta_1}$, where $\xi_{\Delta_1} \in \mathbb{R}^+$ is a positive constant, since the regression vector Ψ_{1f} is locally bounded and Δ_1 is bounded. Substituting the linearized form (3) into system dynamics (2), and substituting equation (23), (26) into (27), yields

$$Q_1 = P_1 \theta_1 - \bar{\Delta}_1 \quad (30)$$

Then the estimation error is extracted by defining $H_1 \in \mathbb{R}$ as

$$H_1 \triangleq P_1 \hat{\theta}_1 - Q_1 \quad (31)$$

which contains the estimation error $\tilde{\theta}_1$ as

$$H_1 = -P_1 \tilde{\theta}_1 + \bar{\Delta}_1 \quad (32)$$

is derived by substituting equation (30) into (31).

Based on the extracted estimation error above, the parameter update law can be designed as

$$\dot{\hat{\theta}}_1 = -\gamma(\gamma_1 H_1 + \text{sat}(H_1)) \quad (33)$$

where $\gamma, \gamma_1 \in \mathbb{R}^+$ are positive learning gains and the saturation function $\text{sat}(\cdot) : \mathbb{R} \rightarrow \mathbb{R}$ is defined as

$$\text{sat}(x) = \begin{cases} 1, & x > 1 \\ x, & |x| \leq 1 \\ -1, & x < -1 \end{cases} \quad (34)$$

B. Estimation In Inner-Loop

In the same manner as estimation in outer-loop, filtered auxiliary vectors $\Psi_{2f} \in \mathbb{R}^{3 \times 3}$, R_f and $\Delta_{2f} \in \mathbb{R}^3$ are defined by the following differential equations:

$$\begin{cases} \alpha_2 \dot{\tau}_{Bf} + \tau_{Bf} = \tau_B, & \tau_{Bf}(0) = \mathbf{0} \\ \alpha_2 \dot{\Psi}_{2f} + \Psi_{2f} = \Psi_2, & \Psi_{2f}(0) = \mathbf{0} \\ \alpha_2 \dot{\Delta}_{2f} + \Delta_{2f} = \Delta_2, & \Delta_{2f}(0) = \mathbf{0} \end{cases} \quad (35)$$

where $\alpha_2 \in \mathbb{R}^+$ is a designed constant. For estimation error extraction, $P_2 \in \mathbb{R}^{3 \times 3}$, $Q_2 \in \mathbb{R}^3$, and $\bar{\Delta}_2 \in \mathbb{R}^3$ are defined as

$$\begin{cases} P_2 \triangleq \int_0^t e^{-l_2(t-\tau)} \Psi_{2f}^T(\tau) \Psi_{2f}(\tau) d\tau + \varrho_2 E_3 \\ Q_2 \triangleq \int_0^t e^{-l_2(t-\tau)} \Psi_{2f}^T(\tau) \tau_{Bf}(\tau) d\tau \\ \bar{\Delta}_2 \triangleq - \int_0^t e^{-l_2(t-\tau)} \Psi_{2f}^T(\tau) \Delta_2 d\tau + \varrho_2 E_3 \theta_2 \end{cases} \quad (36)$$

where $l_2, \varrho_2 \in \mathbb{R}^+$ are designed positive constants and $E_3 \in \mathbb{R}^{3 \times 3}$ is the identity matrix. $\bar{\Delta}_2$ is bounded by $\|\bar{\Delta}_2\| \leq \xi_{\Delta_2}$. Similar to P_1 , P_2 has the following property:

Property 4. P_2 is a positive definite matrix satisfying $0 < \varrho_2 < \lambda_m(P_2)$ where $\lambda_m(P_2)$ is the minimum eigenvalue of P_2 . And P_2^{-1} is globally invertible.

Define $H_2 \in \mathbb{R}^3$ as

$$H_2 \triangleq P_2 \hat{\theta}_2 - Q_2 \quad (37)$$

which yields

$$H_2 = -P_2 \tilde{\theta}_2 + \bar{\Delta}_2 \quad (38)$$

in the same manner as estimation in outer-loop. The parameter update law for inner-loop can be designed as

$$\dot{\hat{\theta}}_2 = -\Gamma \left(\sigma_1 H_2 + \sigma_1 \frac{P_2^T H_2}{\|P_2\|} + \sigma_2 \frac{P_2^T H_2}{\|P_2\| \cdot \|H_2\|} \right) \quad (39)$$

where $\Gamma \in \mathbb{R}^{3 \times 3}$ is a positive definite diagonal matrix, and $\sigma_1, \sigma_2 \in \mathbb{R}^+$ are positive constants.

V. STABILITY ANALYSIS

The stability analysis for the proposed method is conducted in two parts: outer-loop and inner-loop. Both controllers yields asymptotic convergence of tracking error and finite time convergence of estimation error.

A. Inner-Loop Analysis

To facilitate stability analysis of inner-loop, the time derivative of equation (22) is exploited:

$$J\dot{r}_i = \tilde{N}_i + N_{\Delta_i} - \dot{\mu}_2 - e_{i2} \quad (40)$$

In equation (40), part of the equation is separated into two unmeasurable auxiliary functions $\tilde{N}_i, N_{\Delta_i} \in \mathbb{R}^3$ which are upper-bounded by different terms. The motivation for such operation has been discussed in [29]. Substituting equation (39) into equation (40), \tilde{N}_i and N_{Δ_i} can be defined as

$$\begin{aligned} \tilde{N}_i(t) &\triangleq \dot{S}_2 + e_{i2} + N_i \\ N_{\Delta_2} &\triangleq \dot{\Delta}_2 \end{aligned} \quad (41)$$

where $N_i \in \mathbb{R}^3$ is another auxiliary function defined as

$$N_i \triangleq \Psi_{2d} \tilde{\theta}_2 - \Psi_{2d} \dot{\tilde{\theta}}_2 \quad (42)$$

As is discussed in [27], \tilde{N}_i is upper bounded as follows:

$$\|\tilde{N}_i\| \leq \rho(\|z_i\|) \|z_i\| \quad (43)$$

where the outer-loop error signal $z_i \in \mathbb{R}^{12}$ is defined as

$$z_i \triangleq \begin{bmatrix} e_{i1}^T & e_{i2}^T & r_i^T & \tilde{\theta}_2^T \end{bmatrix}^T \quad (44)$$

and $\rho: \mathbb{R}_{\geq 0} \rightarrow \mathbb{R}_{\geq 0}$ is a globally invertible, nondecreasing function. From Assumption 1, $\|N_{\Delta_i}\|$ and $\|\tilde{N}_{\Delta_i}\|$ are bounded by positive constants:

$$\|N_{\Delta_i}\| \leq \xi_i, \quad \|\tilde{N}_{\Delta_i}\| \leq \dot{\xi}_i \quad (45)$$

Lemma 1. Let the auxiliary function $L_i(t) \in \mathbb{R}$ be defined as follows:

$$L_i(t) \triangleq r_i^T (N_{\Delta_i} - \beta_i \text{sgn}(e_{i2})) + C_i \quad (46)$$

If the control gain β_i is selected to fulfill the following condition:

$$\beta_i > \xi_i + \frac{1}{k_{i2}} \dot{\xi}_i \quad (47)$$

and $C_i \in \mathbb{R}^+$ is defined as

$$C_i \triangleq \sigma_1 \left(\frac{1}{\lambda_i} + \frac{1}{\varrho_2} \right) \xi_{\Delta_2}^2 + \sigma_2 \frac{1}{\varrho_2} \xi_{\Delta_2} \quad (48)$$

where $\lambda_i < \varrho_2$ is a positive constant. Then $W_i \in \mathbb{R}$ defined by the following differential equation is always positive:

$$\begin{aligned} \dot{W}_i &\triangleq -\dot{L}_i \\ W_i(0) &\triangleq \beta_i |e_{i2}(0)| - e_{i2}(0) N_{\Delta_i}(0) \end{aligned} \quad (49)$$

The proof of Lemma 1 is similar to that given in [23] and [27].

Theorem 1. The inner-loop controller given in equation (19), (20), and (39) ensures that signal z_i is regulated that $\|z_i(t)\| \rightarrow 0$ as $t \rightarrow \infty$ provided that control gain k_{s2} is selected sufficiently large, $k_{i1}, k_{i2} > \frac{1}{2}$, and β_i following the condition (47).

Proof. Define an auxiliary vector $y \in \mathbb{R}^{13}$ as

$$y \triangleq \begin{bmatrix} z_i^T & \sqrt{W_i} \end{bmatrix}^T \quad (50)$$

and let $\mathcal{D} \subset \mathbb{R}^{13}$ be a domain containing $y(t) = \mathbf{0}$. Define a Lyapunov function candidate as

$$V_1(y, t) \triangleq \frac{1}{2} e_{i1}^T e_{i1} + \frac{1}{2} e_{i2}^T e_{i2} + \frac{1}{2} r_i^T J r_i + W_i + \frac{1}{2} \tilde{\theta}_i^T \Gamma^{-1} \tilde{\theta}_2 \quad (51)$$

where $V_1(y, t) : \mathcal{D} \rightarrow \mathbb{R}$ is a positive definite, continuously differentiable function which satisfies

$$U_1(y) \leq V_1(y, t) \leq U_2(y) \quad (52)$$

In equation (52), $U_1(y), U_2(y) \in \mathbb{R}$ are continuous positive definite functions which are defined as

$$\begin{aligned} U_1(y) &\triangleq c_1 \|y\|^2 \\ U_2(y) &\triangleq c_2 \|y\|^2 \end{aligned} \quad (53)$$

where $c_1, c_2 \in \mathbb{R}^+$ are defined as

$$\begin{aligned} c_1 &\triangleq \frac{1}{2} \min\{1, \underline{J}, \bar{\Gamma}^{-1}\} \\ c_2 &\triangleq \frac{1}{2} \max\{1, \bar{J}, \underline{\Gamma}^{-1}\} \end{aligned} \quad (54)$$

In (54), \bar{J} and \underline{J} indicate the maximum and minimum element of the diagonal matrix J respectively. The time derivative of $V_1(y, t)$ in (51) is expressed as

$$\dot{V}_1 = e_{i1}^T \dot{e}_{i1} + e_{i2}^T \dot{e}_{i2} + r_i^T J \dot{r}_i + \dot{W}_i + \tilde{\theta}_2^T \Gamma^{-1} \dot{\tilde{\theta}}_2 \quad (55)$$

Substituting equation (16) and (40) into the time derivative above, one has

$$\begin{aligned} \dot{V}_1 &= e_{i1}^T (e_{i2} - k_{i1} e_{i1}) + e_{i2}^T (r_i - k_{i2} e_{i2}) + \dot{W}_i + \tilde{\theta}_1^T \Gamma^{-1} \dot{\tilde{\theta}}_2 \\ &\quad + r_i^T (\tilde{N}_i(t) + N_{\Delta_i} - \dot{\mu}_2 - e_{i2}) \end{aligned} \quad (56)$$

With the definition of μ_2 in (21) and W_i in (49), some of the terms in (56) can be eliminated, which yields

$$\begin{aligned} \dot{V}_1 &= -k_{i1} e_{i1}^2 - k_{i2} e_{i2}^2 + e_{i1}^T e_{i2} - (k_{s2} + 1) r_i^2 + r_i^T \tilde{N}_i(t) \\ &\quad - C_i + \tilde{\theta}_2^T \Gamma^{-1} \dot{\tilde{\theta}}_2 \end{aligned} \quad (57)$$

From equation (39) and the definition of $\tilde{\theta}_2$, the time derivative of $\tilde{\theta}_2$ is expressed as

$$\dot{\tilde{\theta}}_2 = \Gamma \left(\sigma_1 H_2 + \sigma_1 \frac{P_2^T H_2}{\|P_2\|} + \sigma_2 \frac{P_2^T H_2}{\|P_2\| \cdot \|H_2\|} \right) \quad (58)$$

Then (57) is expressed as

$$\begin{aligned}\dot{V}_1 = & -k_{i1}e_{i1}^2 - k_{i2}e_{i2}^2 + e_{i1}^T e_{i2} - (k_{s2} + 1)r_i^2 + r_i^T \tilde{N}_i(t) \\ & - C_i + \tilde{\theta}_2^T \left(\sigma_1 H_2 + \sigma_1 \frac{P_2^T H_2}{\|P_2\|} + \sigma_2 \frac{P_2^T H_2}{\|P_2\| \cdot \|H_2\|} \right) \\ = & -k_{i1}e_{i1}^2 - k_{i2}e_{i2}^2 + e_{i1}^T e_{i2} - (k_{s2} + 1)r_i^2 + r_i^T \tilde{N}_i(t) \\ & - C_i - \sigma_1 \tilde{\theta}_2^T (P_2 \tilde{\theta}_2 - \bar{\Delta}_2) - \sigma_1 \frac{(H_2 - \bar{\Delta}_2)^T H_2}{\|P_2\|} \\ & - \sigma_2 \frac{(H_2 - \bar{\Delta}_2)^T H_2}{\|P_2\| \cdot \|H_2\|}\end{aligned}\quad (59)$$

By using Young's inequality and the bound of $\tilde{N}_i(t)$ in (43), the following expressions are yielded

$$\begin{aligned}e_{i1}^T e_{i2} & \leq \frac{1}{2}(\|e_{i1}\|^2 + \|e_{i2}\|^2) \\ r_i^T \tilde{N}_i(t) & \leq k_{s2}\|r_i\|^2 + \frac{1}{4k_{s2}}\rho^2(\|z_i\|)\|z_i\|^2 \\ -\sigma_1 \tilde{\theta}_2^T (P_2 \tilde{\theta}_2 - \bar{\Delta}_2) - \sigma_1 \frac{(H_2 - \bar{\Delta}_2)^T H_2}{\|P_2\|} - \sigma_2 \frac{(H_2 - \bar{\Delta}_2)^T H_2}{\|P_2\| \cdot \|H_2\|} \\ & \leq -\sigma_1(\varrho_2 - \lambda_i)\|\tilde{\theta}_2\|^2 + C_i\end{aligned}\quad (60)$$

Substituting (60), (59) is upper bounded as

$$\begin{aligned}\dot{V}_1 & \leq -(k_{i1} - \frac{1}{2})\|e_{i1}\|^2 - (k_{i2} - \frac{1}{2})\|e_{i2}\|^2 - \|r_i\|^2 \\ & \quad + \frac{1}{4k_{s2}}\rho^2(\|z_i\|)\|z_i\|^2 - \sigma_1(\varrho_2 - \lambda_i)\|\tilde{\theta}_2\|^2 \\ & \leq -\left(c_3 - \frac{1}{4k_{s2}}\rho^2(\|z_i\|)\right)\|z_i\|^2\end{aligned}\quad (61)$$

where $c_3 \in \mathbb{R}$ is defined as

$$c_3 \triangleq \min\left\{k_{i1} - \frac{1}{2}, k_{i2} - \frac{1}{2}, 1, \sigma_1(\varrho_2 - \lambda_i)\right\}\quad (62)$$

c_3 is positive provided the definition of λ_i in Lemma 1. The expression in (61) can be further upper bounded as

$$\dot{V}_1 \leq -c_i\|y\|^2, \quad \forall y \in \mathcal{D}_1\quad (63)$$

for some positive constant c_i . Set $\mathcal{D}_1 \subset \mathcal{D}$ is defined as

$$\mathcal{D}_1 \triangleq \{y(t) \in \mathbb{R}^{13} \mid \|y(t)\| \leq \rho^{-1}(2\sqrt{c_3 k_{s2}})\}\quad (64)$$

The inequality (64) shows that $V_1(y, t) \in \mathcal{L}_\infty$ in \mathcal{D}_1 ; hence e_{i1} , e_{i2} , r_i , and $\tilde{\theta}_2 \in \mathcal{L}_\infty$ in \mathcal{D}_1 . Similar to proof in [24], The attraction region $\mathcal{R}_1 \subset \mathcal{D}_1$ as

$$\mathcal{R}_1 \triangleq \left\{y(t) \in \mathbb{R}^{13} \mid U_2(y) \leq c_1 \left(\rho^{-1}(2\sqrt{c_3 k_{s2}})\right)^2\right\}\quad (65)$$

Hence, $\|y(t)\| \rightarrow 0$ as $t \rightarrow \infty, \forall y(0) \in \mathcal{R}_1$, which further indicates that $\|z_i(t)\| \rightarrow 0$ as $t \rightarrow \infty, \forall y(0) \in \mathcal{R}_1$.

Corollary 1. P_2 is upper bounded by $\|P_2\| \leq \xi_{p2}$, where $\xi_{p2} \in \mathbb{R}^+$ is a positive constant.

Proof. From Theorem 1, $\|e_{i1}\| \rightarrow 0$ as $t \rightarrow 0$. Since $\|\Psi_{2d}\|$ is bounded in Property 1, the continuous function Ψ_{2f} is upper bounded by $\|\Psi_{2f}\| \leq \zeta_2$, where $\xi_2 \triangleq \frac{1}{l_2}\zeta_2^2 + \|\varrho_2\| \in \mathbb{R}^+$ is a positive constant. From equation (36),

$$\|P_2\| = e^{-l_2 t} \left\| \int_0^t e^{l_2 \tau} \Psi_{2f}^T(\tau) \Psi_{2f}(\tau) d\tau \right\| + \|\varrho_2 E_3\| \quad (66)$$

The norm of P_2 is upper bounded by

$$\begin{aligned}\|P_2\| & \leq e^{-l_2 t} \zeta_2^2 \int_0^t e^{l_2 \tau} d\tau + \varrho_2 \\ & \leq \frac{1}{l_2} \zeta_2^2 + \varrho_2\end{aligned}\quad (67)$$

The corollary is proved.

Theorem 2. For error system (40) with the adaptive estimation law given in (39), the estimation error variable $P_2^{-1}H_2$ is regulated that $\|P_2^{-1}H_2\| \rightarrow 0$ in a finite time t_1 if Γ , σ_1 , σ_2 and ϱ_2 are properly selected (see the subsequent proof). And the estimation error $\tilde{\theta}_2$ is guaranteed to converge to a compact set around zero in t_i .

Proof. Let $\Xi \subset \mathbb{R}^3$ be a domain containing $\|P_2^{-1}(t)H_2(t)\| = 0$. Define a Lyapunov candidate as

$$V_2(P_2^{-1}H_2) \triangleq \frac{1}{2}H_2^T P_2^{-1} P_2^{-1} H_2 \quad (68)$$

where $V_2(P_2^{-1}H_2) : \Xi \rightarrow \mathbb{R}_{\geq 0}$ is a positive definite, continuously differentiable function satisfies a similar condition to (52). The time derivative of V_2 is expressed as

$$\dot{V}_2 = H_2^T P_2^{-1} \frac{\partial}{\partial t} (P_2^{-1} H_2) \quad (69)$$

From equation (38), one has

$$P_2^{-1} H_2 = -\tilde{\theta}_2 + P_2^{-1} \bar{\Delta}_2 \quad (70)$$

Exploiting $\frac{\partial}{\partial t} P_2^{-1} = -P_2^{-1} \dot{P}_2 P_2^{-1}$, and substituting equation (58) and (70) into (69), \dot{V}_2 can be expressed as

$$\begin{aligned}\dot{V}_2 = & -H_2^T P_2^{-1} \left(\Gamma \sigma_1 H_2 + \Gamma \sigma_1 \frac{P_2^T H_2}{\|P_2\|} \right) \\ & - H_2^T P_2^{-1} \left(\Gamma \sigma_2 \frac{P_2^T H_2}{\|P_2\| \cdot \|H_2\|} - \Phi \right)\end{aligned}\quad (71)$$

where $\Phi \in \mathbb{R}^3$ is defined as

$$\Phi \triangleq -P_2^{-1} \dot{P}_2 P_2^{-1} \bar{\Delta}_2 + P_2^{-1} \dot{\bar{\Delta}}_2 \quad (72)$$

From Assumption 2, Property 4, and Corollary 1, Φ is verified to be bounded, and \dot{V}_2 is upper bounded as

$$\begin{aligned}\dot{V}_2 & \leq -\left(\Gamma \sigma_2 \frac{1}{\xi_{p2}} - \frac{1}{\varrho_2} \|\Phi\|\right) \|H_2\| - \frac{2}{\xi_{p2}} \Gamma \sigma_1 \|H_2\|^2 \\ & \leq -\sqrt{2} \varrho_2 \left(\Gamma \sigma_2 \frac{1}{\xi_{p2}} - \frac{1}{\varrho_2} \|\Phi\| \right) \sqrt{V_2} - 4 \frac{\varrho_2^2}{\xi_{p2}^2} \Gamma \sigma_1 V_2\end{aligned}\quad (73)$$

If σ_2 is selected sufficiently large and Γ , ϱ_2 are selected to satisfy

$$\Gamma \sigma_2 \frac{1}{\xi_{p2}} - \frac{1}{\varrho_2} \|\Phi\| > 0 \quad (74)$$

the expression in (73) can be further upper bounded as

$$\dot{V}_2 \leq -c_{i1} \sqrt{V_2} - c_{i2} V_2, \quad \forall P_2^{-1} H_2 \in \Xi_1 \quad (75)$$

where $c_{i1}, c_{i2} \in \mathbb{R}^+$ are positive constants, and Ξ_1 can be made arbitrarily large by increasing σ_2 and select Γ , ϱ_2 based on the design criteria in (74). Similar to the proof of Theorem 1, an attraction region $\mathcal{R}_\Xi \subset \Xi_1$ exists that $\|P_2^{-1}(t)H_2(t)\| \rightarrow 0$

in $t_i \leq \frac{2}{c_{i2}} \ln(1 + \frac{c_{i2}}{c_{i1}} a_i)$, $\forall P_2^{-1}(0)H_2(0) \in \mathcal{R}_\Xi$ where $a_i \in \mathbb{R}^+$ is defined as $a_i \triangleq \frac{\sqrt{2}}{2} (\|\tilde{\theta}_2(0)\| + \frac{1}{\varrho_2} \xi_{\Delta_2})$.

From the definition of H_2 in equation(38), this further implies that $\tilde{\theta}_2$ converges to a compact set \mathcal{R}_i in t_i , where $\mathcal{R}_i \subset \mathbb{R}^3$ is defined as

$$\mathcal{R}_i \triangleq \left\{ \tilde{\theta}_2(t) \in \mathbb{R}^3 \mid \|\tilde{\theta}_2\| \leq \frac{1}{\varrho_2} \xi_{\Delta_2} \right\} \quad (76)$$

This completes the proof.

Notice that though the FT convergence can be guaranteed by properly selecting Γ , σ_2 , and ϱ_2 while σ_1 is selcted as zero, the selection of learning gain σ_1 also influences the convergence rate of $\|P_2^{-1}H_2\|$. A large σ_1 leads to a faster convergence. However, it might also cause oscillations in the estimated parameters if σ_1 is designed too large.

B. Outer-Loop Analysis

The time derivative of equation (11) is calculated similar to (40) as

$$J\dot{r}_o = \tilde{N}_o + N_{\Delta_1} - \dot{\mu}_1 - e_{o2} \quad (77)$$

where auxiliary functions $\tilde{N}_o, N_{\Delta_1} \in \mathbb{R}^3$ are defined similar to (41). The inner loop error signal $z_o \in \mathbb{R}^{10}$ is defined as

$$z_o \triangleq \begin{bmatrix} e_{o1}^T & e_{o2}^T & r_o^T & \tilde{\theta}_1 \end{bmatrix}^T \quad (78)$$

The subsequent theorems can be proved.

Theorem 3. The outer-loop controller given in equation (8), (9), and (33) ensures that signal z_o is regulated that $\|z_o(t)\| \rightarrow 0$ as $t \rightarrow \infty$ provided that control gain k_{s1} is selected sufficiently large, $k_{o1}, k_{o2} > \frac{1}{2}$, and β_o following a condition similar to (47).

Theorem 4. For error system (77) with the adaptive estimation law given in (33), the estimation error variable $P_1^{-1}H_1$ is regulated that $\|P_1^{-1}H_1\| \rightarrow 0$ in a finite time t_o satisfying $t_o \leq \frac{2}{c_{o2}} \ln(1 + \frac{c_{o2}}{c_{o1}} a_o)$ if γ, γ_1 , and ϱ_1 are properly selected, where $a_o \in \mathbb{R}$ is defined as $a_o \triangleq \frac{\sqrt{2}}{2} (\tilde{\theta}_1(0) + \frac{1}{\varrho_1} \xi_{\Delta_1})$. And $\tilde{\theta}_1$ is guaranteed to converge to a compact set around zero in t_o .

Proof of Theorem 3 and 4. Noticing that $\text{sat}(H_1) \leq 1$, the proof can be conducted in a similar method as that of the inner-loop controller.

VI. SIMULATION

In this section, the effectiveness of the designed controller is verified by simulations and experiments. Comparative simulations are carried out between the proposed strategy and the traditional methods based on SMC and gradient algorithms in [13]. The results show that the proposed method yields better tracking error and estimation convergence. Meanwhile, it generates smoother input signals for practical applications than SMC controllers. The results indicate the robustness against disturbances and mass-inertia changes of the controller.

To verify the performance of the proposed control strategy, numerical simulations are conducted in MATLAB. Table (I) shows the preset mass-inertia parameters of the UAV in simulation. The control gains and learning gains of the proposed RISE-based adaptive controller with mass-inertia

Item	Quantity	Unit
m	3.12	kg
I_x	0.1	$\text{kg} \cdot \text{m}^2$
I_y	0.1	$\text{kg} \cdot \text{m}^2$
I_z	0.2	$\text{kg} \cdot \text{m}^2$

TABLE I
TRUE VALUE OF MASS-INERTIA PARAMETERS

estimation (RISE-Emi) is selected as the following table (II). And the learning gain matrix Γ is selected as

$$\Gamma = \begin{bmatrix} 10^{-4} & 0 & 0 \\ 0 & 10^{-4} & 0 \\ 0 & 0 & 4.5 \times 10^{-3} \end{bmatrix} \quad (79)$$

Outer-loop gains		Inner-loop gains	
Symbol	Value	Symbol	Value
k_{o1}	1	k_{i1}	2
k_{o2}	1	k_{i2}	1
k_{s1}	5.4	k_{s2}	4.5
β_o	1	β_i	1
α_1	3	α_2	5
ϱ_1	0.5	ϱ_2	0.5
γ	0.3	σ_1	8
γ_1	0.17	σ_2	200

TABLE II
TABLE: CONTROL AND LEARNING GAINS

The comparison is conducted between RISE-Emi and the adaptive sliding mode controller with gradient-based mass estimation (ASMC) proposed in [13]. We selct the desired trajectry and yaw angle as

$$\begin{aligned} \eta_{1d} &= 2\sin(t) \cdot \begin{bmatrix} 1 & 1 & 1 \end{bmatrix}^T \\ \psi_d &= \sin(1.1t) \end{aligned} \quad (80)$$

and add white noise disturbance to the dynamic model output of the system.

The result of mass-inertia estimation of RISE-Emi is show in Fig. 2. The initial estimation of mass is set 50% smaller than the real value, and the initial inertia estimations are about 100%, 100% and 50% larger respectively. All 4 estimated values converge to its truth finally. Due to the different dynamic characters between yaw orientation and roll, pitch orientation, the estimation of I_z overshoots for about 5% with the selected parameters. And the convergence of mass is relatively slow because of the slower response of the outer loop compared to the inner loop. Meanwhile, the estimation error is compared with the mass estimation of ASMC in Fig. 3. Initially, the estimated mass of the 2 methods converge at a similar speed. Then, the estimation in RISE-Emi achieves the 2% bound faster, and gradually reaches the real value within about 10s, while keeps increasing at a large speed and saturates before convergence in ASME. It is also noticable that because of the added white noise, the steady-state error can not be zero all the time. However, the error caused by

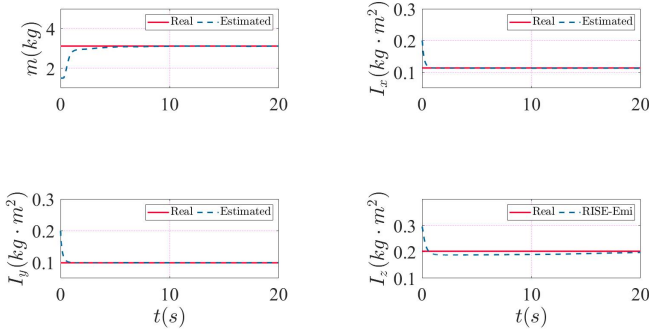


Fig. 2. Parameter estimation results

the noise in RISE-Emi is smaller than that of ASMC, which is shown in the sub-figure of Fig. 3.

These results indicate the effectiveness of our method in mass-inertia estimation and its robustness against disturbances.

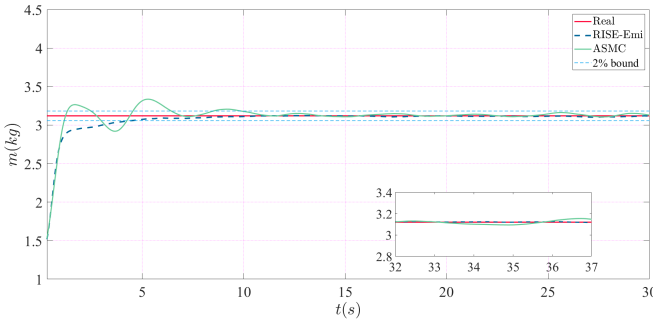


Fig. 3. Comparison of estimation of mass

Then, the comparison of trajectory and attitude tracking errors are provided in Fig. 4. and Fig. 5 respectively. The trajectory tracking errors increase greatly in the beginning mainly because of the imprecise initial estimation, which undermines the performance of the controllers. Then, the tracking errors of the proposed method converge faster than ASMC, also yielding smaller steady-state errors in x and y directions. And it is obvious that the scale of attitude tracking error in RISE-Emi is much smaller, which illustrate the disturbance rejection ability of our method.

Finally, the thrust output of the controller is compared in Fig. 6. The output of the proposed method is smoother than that of ASMC when disturbance exists, which is more physically achievable in practical applications.

VII. CONCLUSION

In this work, we have developed and validated an adaptive control strategy for UAVs in face of external disturbances and mass-inertia variation. First, a dynamic model of multi-rotor UAVs with disturbances is derived with a linearly parameterized form. Then, a cascade control law is designed based on this form with robust RISE terms. Finally, mass-inertia estimation is conducted based on a filtering operation to improve the robustness against possible mass-inertia

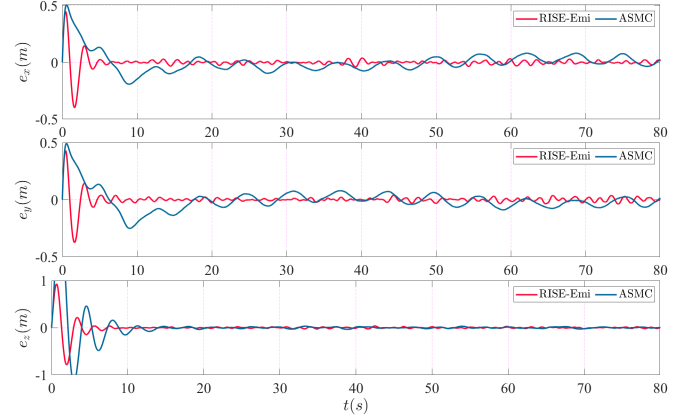


Fig. 4. Position tracking errors

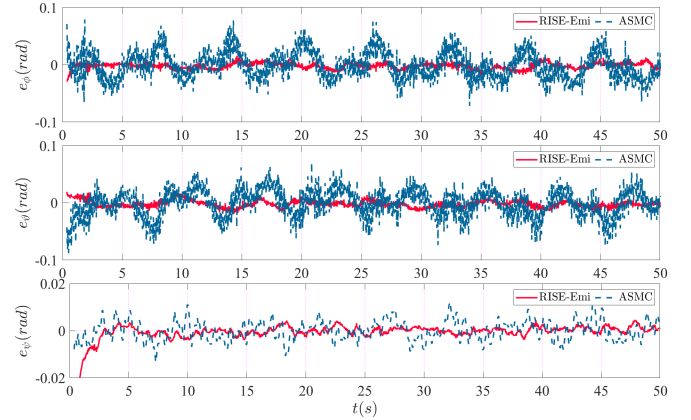


Fig. 5. Attitude tracking errors

change. Comparative simulations have shown that a better performance can be achieved with our method than the previously proposed method ASMC.

ACKNOWLEDGEMENT

This work is motivated by Haoxuan Shan's work of a integrated quadrupe-hexarotor system. Gang Chen has also contributed to the idea and process of the research.

REFERENCES

- [1] M. Hochstenbach, C. Notteboom, B. Theys, and J. D. Schutter, "Design and control of an unmanned aerial vehicle for autonomous parcel delivery with transition from vertical take-off to forward flight – vertikul, a quadcopter tailsitter," *International Journal of Micro Air Vehicles*, vol. 7, no. 4, pp. 395–405, 2015. [Online]. Available: <https://doi.org/10.1260/1756-8293.7.4.395>
- [2] H. Shan, G. Chen, S. Shi, Z. W. Maoshen Qin, and W. Dong, "Dragon rider - an integrated unmanned quadrupe-hexarotor system for flight-impeded area exploration," in *2021 27th International Conference on Mechatronics and Machine Vision in Practice (M2VIP)*, 2021, pp. 411–416.
- [3] X. Liang, G. Chen, J. Wang, Z. Bi, and P. Sun, "An adaptive control system for variable mass quad-rotor uav involved in rescue missions," *International Journal of Simulation Systems, Science and Technology*, vol. 17, pp. 22.1–22.7, 01 2016.
- [4] N.-S. Kim and T.-Y. Kuc, "Sliding mode backstepping control for variable mass hexa-rotor uav," in *2020 20th International Conference on Control, Automation and Systems (ICCAS)*, 2020, pp. 873–878.

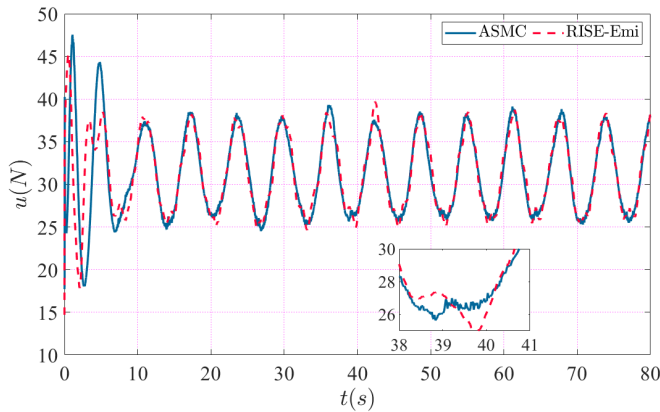


Fig. 6. Comparison of thrust

- [5] Z. T. Dydek, A. M. Annaswamy, and E. Lavretsky, "Adaptive control of quadrotor uavs: A design trade study with flight evaluations," *IEEE Transactions on Control Systems Technology*, vol. 21, no. 4, pp. 1400–1406, 2013.
- [6] B. H. Wang, D. B. Wang, Z. A. Ali, B. T. Ting, and H. Wang, "An overview of various kinds of wind effects on unmanned aerial vehicle," *Measurement and Control*, vol. 52, no. 7-8, pp. 731–739, 2019. [Online]. Available: <https://doi.org/10.1177/0020294019847688>
- [7] P. Pounds, D. Bersak, and A. Dollar, "Stability of small-scale uav helicopters and quadrotors with added payload mass under pid control," *Autonomous Robotics*, vol. 33, pp. 129–142, 2012. [Online]. Available: <https://doi.org/10.1007/s10514-012-9280-5>
- [8] I. Sadeghzadeh, M. Abdolhosseini, and Y. Zhang, "Payload drop application using an unmanned quadrotor helicopter based on gain-scheduled pid and model predictive control," *Unmanned Systems*, vol. 02, no. 01, pp. 39–52, 2014. [Online]. Available: <https://doi.org/10.1142/S2301385014500034>
- [9] A. Parsa, S. B. Monfared, and A. Kalhor, "Backstepping control based on sliding mode for station-keeping of stratospheric airship," in *2018 6th RSI International Conference on Robotics and Mechatronics (ICRoM)*, 2018, pp. 554–559.
- [10] Z. Zhao, D. Cao, J. Yang, and H. Wang, "High-order sliding mode observer-based trajectory tracking control for a quadrotor uav with uncertain dynamics," *Nonlinear Dynamics*, vol. 102, no. 4, pp. 2583–2596, 12 2020. [Online]. Available: <https://www.proquest.com/scholarly-journals/high-order-sliding-mode-observer-based-trajectory/docview/2473334526/se-2?accountid=13818>
- [11] L. Zhou, S. Xu, H. Jin, and H. Jian, "A hybrid robust adaptive control for a quadrotor uav via mass observer and robust controller," *Advances in Mechanical Engineering*, vol. 13, no. 3, p. 16878140211002723, 2021. [Online]. Available: <https://doi.org/10.1177/16878140211002723>
- [12] L. Zhou, J. Zhang, J. Dou, and B. Wen, "A fuzzy adaptive backstepping control based on mass observer for trajectory tracking of a quadrotor uav," *International Journal of Adaptive Control and Signal Processing*, vol. 32, no. 12, pp. 1675–1693, 2018. [Online]. Available: <https://onlinelibrary.wiley.com/doi/abs/10.1002/acs.2937>
- [13] H. Bouadi, A. Aoudjif, and M. Guenifi, "Adaptive flight control for quadrotor uav in the presence of external disturbances," in *2015 6th International Conference on Modeling, Simulation, and Applied Optimization (ICMSAO)*, 2015, pp. 1–6.
- [14] K. S. HATAMLEH, O. MA, and R. PAZ, "A uav model parameter identification method: A simulation study," *International Journal of Information Acquisition*, vol. 06, no. 04, pp. 225–238, 2009. [Online]. Available: <https://doi.org/10.1142/S0219878909001977>
- [15] M. A. Al-Shabi, K. S. Hatamleh, and A. A. Asad, "Uav dynamics model parameters estimation techniques: A comparison study," in *2013 IEEE Jordan Conference on Applied Electrical Engineering and Computing Technologies (AEECT)*, 2013, pp. 1–6.
- [16] D. Mellinger, Q. Lindsey, M. Shomin, and V. Kumar, "Design, modeling, estimation and control for aerial grasping and manipulation," in *2011 IEEE/RSJ International Conference on Intelligent Robots and Systems*, 2011, pp. 2668–2673.
- [17] G. Antonelli, E. Cataldi, F. Arrichiello, P. Robuffo Giordano, S. Chiverini, and A. Franchi, "Adaptive trajectory tracking for quadrotor mavs in presence of parameter uncertainties and external disturbances," *IEEE Transactions on Control Systems Technology*, vol. 26, no. 1, pp. 248–254, 2018.
- [18] I. Palunko and R. Fierro, "Adaptive control of a quadrotor with dynamic changes in the center of gravity," *IFAC Proceedings Volumes*, vol. 44, no. 1, pp. 2626–2631, 2011, 18th IFAC World Congress. [Online]. Available: <https://www.sciencedirect.com/science/article/pii/S1474667016440097>
- [19] Z. Liu, X. Liu, J. Chen, and C. Fang, "Altitude control for variable load quadrotor via learning rate based robust sliding mode controller," *IEEE Access*, vol. 7, pp. 9736–9744, 2019.
- [20] O. Mofid and S. Mobayen, "Adaptive sliding mode control for finite-time stability of quad-rotor uavs with parametric uncertainties," *ISA Transactions*, vol. 72, pp. 1–14, 2018. [Online]. Available: <https://www.sciencedirect.com/science/article/pii/S0019057817306171>
- [21] V. N. Sankaranarayanan, S. Roy, and S. Baldi, "Aerial transportation of unknown payloads: Adaptive path tracking for quadrotors," in *2020 IEEE/RSJ International Conference on Intelligent Robots and Systems (IROS)*, 2020, pp. 7710–7715.
- [22] J. Zhao, X. Ding, B. Jiang, G. Jiang, and F. Xie, "A novel control strategy for quadrotors with variable mass and external disturbance," *International Journal of Robust and Nonlinear Control*, vol. 31, no. 17, pp. 8605–8631, 2021. [Online]. Available: <https://onlinelibrary.wiley.com/doi/abs/10.1002/rnc.5760>
- [23] S. Wang and J. Na, "Parameter estimation and adaptive control for servo mechanisms with friction compensation," *IEEE Transactions on Industrial Informatics*, vol. 16, no. 11, pp. 6816–6825, 2020.
- [24] B. J. Bialy, J. Klotz, K. Brink, and W. E. Dixon, "Lyapunov-based robust adaptive control of a quadrotor uav in the presence of modeling uncertainties," in *2013 American Control Conference*, 2013, pp. 13–18.
- [25] J. Na, M. N. Mahyuddin, G. Herrmann, X. Ren, and P. Barber, "Robust adaptive finite-time parameter estimation and control for robotic systems," *International Journal of Robust and Nonlinear Control*, vol. 25, no. 16, pp. 3045–3071, 2015. [Online]. Available: <https://onlinelibrary.wiley.com/doi/abs/10.1002/rnc.3247>
- [26] K. S. NARENDRA and A. M. ANNASWAMY, "Persistent excitation in adaptive systems," *International Journal of Control*, vol. 45, no. 1, pp. 127–160, 1987. [Online]. Available: <https://doi.org/10.1080/00207178708933715>
- [27] B. Xian, D. Dawson, M. de Queiroz, and J. Chen, "A continuous asymptotic tracking control strategy for uncertain nonlinear systems," *IEEE Transactions on Automatic Control*, vol. 49, no. 7, pp. 1206–1211, 2004.
- [28] D. Mellinger and V. Kumar, "Minimum snap trajectory generation and control for quadrotors," in *2011 IEEE International Conference on Robotics and Automation*, 2011, pp. 2520–2525.
- [29] P. M. Patre, W. MacKunis, K. Dupree, and W. E. Dixon, "Modular adaptive control of uncertain euler-lagrange systems with additive disturbances," *IEEE Transactions on Automatic Control*, vol. 56, no. 1, pp. 155–160, 2011.